

Article

Finite Elements Analysis of Biomechanical Behavior of the Bracket in a Gradual Horizontal Periodontal Breakdown—A Comparative Analysis of Multiple Failure Criteria

Radu Andrei Moga ^{1,*}, Cristian Doru Olteanu ^{2,*}, Stefan Marius Buru ³, Mircea Daniel Botez ³
and Ada Gabriela Delean ¹

¹ Department of Cariology, Endodontics and Oral Pathology, School of Dental Medicine, University of Medicine and Pharmacy Iuliu Hatieganu, Str. Motilor 33, 400001 Cluj-Napoca, Romania; ada.delean@umfcluj.ro

² Department of Orthodontics, School of Dental Medicine, University of Medicine and Pharmacy Iuliu Hatieganu, Cluj-Napoca, Str. Avram Iancu 31, 400083 Cluj-Napoca, Romania

³ Department of Structural Mechanics, School of Civil Engineering, Technical University of Cluj-Napoca, Str. Memorandumului 28, 400114 Cluj-Napoca, Romania; marius.buru@mecon.utcluj.ro (S.M.B.); mircea.botez@mecon.utcluj.ro (M.D.B.)

* Correspondence: andrei.moga@umfcluj.ro (R.A.M.); olteanu.cristian@umfcluj.ro (C.D.O.)

Featured Application: Patients suffering from various levels of periodontal breakdown show increased problems related to the amount of orthodontic force (usually light) needed to be safely applied to minimize ischemic, necrotic, resorptive, and further periodontal loss risks. At the bracket level, the bond failure risk is another issue that must be addressed. This study helps practitioners regarding the biomechanical stress distribution in both the stainless-steel bracket (commonly used in daily practice) and the enamel component, proving a non-homogenous stress distribution nature and a lack of influence of the periodontal breakdown process over this stress distribution. From a scientific point of view, both practitioners and researchers have a clearer image about the biomechanical behavior of the stress distribution in periodontal breakdown simulation (with this being the first study to address this issue) and are provided with a more comprehensive modality to understand the finite element analysis principles and the correct selection and use of different failure criteria.

Abstract: This study assessed the stress distribution (in eighty-one 3D models of the second lower premolar) in a stainless-steel bracket and enamel crown under 0.5 N of intrusion, extrusion, rotation, translation, and tipping during a horizontal periodontal breakdown of 0–8 mm. The FEA simulations (totaling 405) employed five failure criteria and assessed the adequacy and accuracy of Von Mises (VM), Tresca (T), Maximum Principal (S1), Minimum Principal (S3), and Hydrostatic Pressure. T and VM criteria showed no change in stress display areas during the periodontal breakdown, seeming to be more correct and adequate than the other three (with unusual stress displays). Both VM and T (found to be more adequate) generated maximum stress areas on the attachment side and the entire base of the bracket, confirming the non-homogenous stress distribution areas and the risks of bond failure. Rotation, translation, and tipping were the most stressful movements and showed slightly lower quantitative values for 8 mm bone loss when compared with the intact periodontium, while intrusion and extrusion showed the opposite behavior (slight increase). Periodontal breakdown did not influence the stress display in the bracket and its surrounding enamel area during the five orthodontic movements.

Keywords: stainless-steel bracket; light orthodontic forces; horizontal periodontal breakdown; FEA analyses; failure criteria; dentistry; orthodontics



Citation: Moga, R.A.; Olteanu, C.D.; Buru, S.M.; Botez, M.D.; Delean, A.G. Finite Elements Analysis of Biomechanical Behavior of the Bracket in a Gradual Horizontal Periodontal Breakdown—A Comparative Analysis of Multiple Failure Criteria. *Appl. Sci.* **2023**, *13*, 9480. <https://doi.org/10.3390/app13169480>

Academic Editor: Andrea Scribante

Received: 20 July 2023

Revised: 11 August 2023

Accepted: 11 August 2023

Published: 21 August 2023



Copyright: © 2023 by the authors. Licensee MDPI, Basel, Switzerland. This article is an open access article distributed under the terms and conditions of the Creative Commons Attribution (CC BY) license (<https://creativecommons.org/licenses/by/4.0/>).

1. Introduction

Many patients suffering from periodontal disease need orthodontic treatment. Nevertheless, a reduction in periodontal support (i.e., bone and periodontal ligament—PDL) affects the biomechanical behavior of the tooth during various orthodontic movements [1–5]. The bracket and enamel components of the tooth are the first to suffer from stresses produced by orthodontic force application.

The most sensitive area is the internal side of the bracket where the bracket–cement–enamel bond/attachment is found and the failure usually occurs (i.e., 6–28.3% of the failure rate, especially in posterior teeth mandibular [1]) [1–5]. Among the consequences of the failure of the bracket bond are the complication of the movements and fine adjustments due to difficulty in finding the original position and angulation of the bracket and the increase in treatment time [1,2]. This type of failure is due to interference with contact loading, incorrect bonding procedures, fatigue of the bonding material, and/or the association of these factors [1,2]. Moreover, the slot walls are also subjected to various forms of deformation that significantly influence the biomechanical stress distribution in the bracket and enamel depending on the bracket and arch materials, geometry, dimensions, and applied forces [5,6]. There are studies [1–7] limited only to the assessment of the stress distribution in the bracket (either in the slot walls or on the attachment/internal side), but no studies describing how the progress of periodontal breakdown influences the stress distribution in the bracket and enamel (or in the tooth and PDL) were found.

A clear image of the stress distribution and dissipation that occurs in the bracket and enamel is possible only via *in vitro* experiments and finite elements analysis (FEA) [1–7]. *In vitro* tests allow us to identify the maximum amount of force to be applied and maximum bond strengths (e.g., brackets attached to various types of surfaces subjected to machine testing loads), but do not provide any data regarding the stress distribution and absorption or the areas suffering from higher stresses (since the bonding area is not equally loaded) [1–3]. There are also reports of variable changes in physical properties of teeth subjected to *in vitro* experiments [8]. Other reports considered FEA analysis to be superior to *in vitro* experiments regarding accuracy due to issues in modeling and validation [9]. On the other hand, FEA studies can accurately reconstruct the anatomical tissues and properties compared with *in vitro* studies where the tooth is integrated with various materials not resembling human tissue [9]. Earlier reports showed that shear, compressive, and tensile stresses are not homogenous, with the weak point being a void, a crack, or the border of the bracket [2,3]. Nevertheless, the FEA method also has limitations, the most significant being that it cannot accurately reproduce the complexity of clinical situations.

Cement is a brittle material that has no elastic deformation, ending rapidly in the fracture and debonding of the bracket [2]. The bracket is made of several types of materials, the most common being stainless steel (a ductile material) and ceramics (a brittle material), which behave completely differently biomechanically when subjected to orthodontic stresses [2,3]. According to the material's yielding theory, the ductile materials have the ability to undergo various reversible elastic deformations (before the plastic one occurs), while the brittle materials suffer directly from various plastic deformations closely followed by buckling (changes in shape under loads) and fracture. Despite the acknowledged engineering data related to the type of material (brittle, ductile, liquid, and gas) with the specific failure criteria, its use in dental studies is almost nonexistent (except for a few studies [10–13]).

Enamel is considered a brittle material due its internal micro-architecture structure, while all tooth components and the surrounding periodontium are of ductile resemblance, having various abilities of absorption and dissipation of loading stresses [7,8,10,11,13–17]. Thus, the entire tooth and support system behave as ductile materials (the stainless-steel bracket included) since the enamel is only an extremely small percentage of the tooth and the periodontium's entire volume [8,13,18]. The ductile resemblance (however, with a certain brittle flow mode) of these structures is supported by the reported absorption–dissipation ability of these tissues [13,15,16].

It would therefore be of clinical importance to have a simulation of stress distribution in bracket and enamel components during the periodontal breakdown process to find the areas with highest stresses for a better understanding of bracket bond failures and their prevention.

FEA allows the individual assessment of stress distribution in the bracket and enamel, but for correct results, the type of analyzed material (ductile or brittle) needs to be considered, since each failure criterion is designed to accurately describe a certain biomechanical behavior. In dental studies the most used failure criteria are the Von Mises (VM) [9,12,19–23] and Tresca (T) [10,11,13,24,25] criteria designed for ductile materials, the Maximum Principal S1 tensile [12,20,26–29] and Minimum Principal S3 compressive [12,26,27,29–32] stresses designed for brittle materials, and Hydrostatic pressure (HP) [33–37] designed for liquids and gases. Additionally, variables such as force levels [38] and mechanical characteristics of orthodontic wires [39] should also be taken into consideration. Nevertheless, there are no studies besides our earlier ones [7,10,11,13,24,25] which address this essential issue for the accuracy of the FEA method.

Current FEA studies of stress distributions in brackets are concentrated on identifying the bond strength of several types of brackets and stresses in bracket–cement–enamel structures [1–3]. FEA analysis is usually used to assess the shear bond strength (i.e., 4–10 MPa of Reynolds) and tensile bond strength (i.e., 6–8 MPa of Reynolds) [1–3], correctly applicable if the analyzed materials are either entirely brittle or ductile. The slot size of the bracket (e.g., reports of 0.018-inch brackets supplying a better torque control than 0.022-inch brackets) and arch diameter, material, and form had equally considerable influence over FEA stress distributions [4]. The bracket slot walls, depending on their design and materials, suffer from several types of deformations [5,6] that could alter FEA results if the entire tooth's biomechanical behavior is not assessed. However, since previous reports [1–6] have only concentrated on assessing a small region of the tooth (i.e., artificially designed and 3D modeled [1–3]) without taking into consideration the analysis of a larger structure, such as the bracket or entire enamel component (i.e., the crown) or tooth and its surrounding supporting structures (improving thus the knowledge), they do not address the problem of selecting the adequate failure criteria in their FEA analyses. Moreover, if analyzed structures are made of different types of materials (i.e., enamel, cement, and ceramic brackets are brittle, while stainless-steel brackets are ductile) in relatively equal percent proportions, the failure criteria must be carefully selected due to their specific mathematical design to better describe the ductile or brittle materials' behaviors [10–13,24,25]. However, if the brittle/ductile material represents only an extremely small percentage of the entire volume of an analyzed structure, the failure criteria that best describe the predominant material's type of structure should be employed [7,10,11,13,24,25].

These FEA studies [1–3] reported that shear loading at the short side of the bracket produced the highest bond strength and lower tensile stress, with ceramic having a higher strength than stainless steel. Moreover, due to the different behavioral mechanical meanings, the tensile bond strength should not be compared with the shear bond strength (Reynolds interval used as reference) [1]. Nevertheless, to find the actual shear bond strength, only pure shear force should be applied directly to bracket–adhesive interface, which is extremely difficult, even in an FEA [1].

Usually in clinical practice, low/light orthodontic forces (0.5–1.2 N) are recommended to be employed, and their efficiency has been clinically proven [17]; meanwhile, the causes of bracket bond failure are more so due to bonding technique problems than to a high amount of applied force (e.g., forces of 10 N). The acknowledged limitations of all these studies [1–3] are that the results are theoretical in nature and reflect an *in vitro* approach [1] (e.g., 10 N stroke applied, while the number of strokes for each bracket failure was found vs. acknowledged clinical behavior). However, this type of approach is far from the reality of clinical biomechanical stress distribution; thus, an approach closer to the reality of clinical mechanical behavioral must be used to assess stress distribution–absorption in both brackets and enamel components. Moreover, not only the light orthodontic force but

also several types of bone loss and the knowledge of biomechanical behavior of the other structural component tissues of the tooth and periodontal support system must be taken into consideration when assessing the stress distribution–absorption mechanism. The tooth and surrounding support tissues are anatomically anisotropic, non-homogenous, and have various properties and biomechanical behaviors (i.e., linear elastic vs. non-linear elastic, varying with amount of applied force) depending on experimental circumstances, and usually do not abide by Hook’s law [8]. Thus, correlating several types of studies (i.e., FEA, in vivo/in vitro) for a better and clearer image of the entire tooth and periodontal system’s biomechanical behavior and addressing the issues of the results’ accuracy is of importance.

Based on the above, the need for a different approach closer to clinical reality in the study of stress distribution is obvious. Thus, the aim of the present study was to assess both stress distribution and absorption–dissipation in the bracket and enamel crown components for lower premolars in the presence of a gradual horizontal breakdown of 0–8 mm and under 0.5 N of intrusion, extrusion, rotation, translation, and tipping. Moreover, shear, overall, tensile, compressive, and pressure stresses were assessed by employing the adequate failure criteria for each of these stresses, thus investigating the failure criteria more suitability for the study of brackets and enamel.

2. Materials and Methods

Herein, a finite elements study is a part of a broader step-by-step research (i.e., clinical protocol 158/02.04.2018) investigating the accuracy of the FEA method in the study of dental structures subjected to orthodontic forces and periodontal breakdown [7,10,11,13,24,25].

This analysis employed eighty-one 3D mesh models (in 405 simulations) of the second lower premolar with surrounding support tissues, reconstructed from the CBCT exams of nine patients (mean age 29.81 ± 1.45 years, four males, five females, with oral informed consent) in need of orthodontic treatment and with various levels of bone loss (usually in cervical third of PDL).

For this research, a higher number of patients was examined, but due to inclusion criteria, only nine qualified. The main inclusion criteria were non-inflamed periodontium, good oral hygiene, intact investigated teeth, no tooth loss in the investigated region, no malposition or unhealthy oral habits, and reduced various bone loss levels. Due to all of the above criteria the sample size of 9 patients (9 patients, 81 models, 405 simulations) considered to be acceptable for the accuracy of results and conclusions, since most of other FEA studies related to bracket and PDL/dental pulp/tooth subjects employed a sample size of one (one model/one patient/few simulations, usually reconstructed based on ideal anatomic dimensions and anatomy, with no anatomical accuracy related to the complexity of human tissues).

The CBCT examinations were performed with ProMax 3DS (Planmeca, FI-00880 Helsinki, Finland), with a 0.075 mm voxel size. The region of interest was the mandibular sector with two premolars and molars.

CBCT images were loaded into Amira 5.4.0 reconstruction software (Visage Imaging Inc., 300 Brickstone Square, Suite 201 Andover, MA 01810, USA) to obtain mesh models. The reconstruction process was manually performed by a single experienced practitioner, since the automated software algorithm met difficulties in finding the limits and small grey shades of dental pulp, PDL, and cementum. Thus, tooth components (enamel, dentine, dental pulp, neurovascular bundle (NVB)), supporting tissues’ periodontal ligaments, and the cortical and trabecular bones were found and reconstructed. The cementum separation from dentine was found to be impossible and was acceptable to be reconstructed as dentine due to their similar physical properties (Table 1).

The bracket (stainless steel) was manually reconstructed in this phase of the study to be able to simulate a close contact to the enamel component (an almost perfect bond), Figure 1H. The slot of the bracket was chosen not to be reconstructed to avoid any problems related to variability in dimensions, angulations, and geometry and to allow orthodontic forces to be directly applied to the base of the bracket. Cutting the deformations of slot

walls due to orthodontic forces (aspect acknowledged in the study) allowed the assessment of total amount of stress directly applied to the base of the bracket (eliminating absorption–dissipation of stresses due to deformations). Clinically, there are no pure orthodontic movements, but rather a combination of them. Thus, in clinical biomechanics, the amounts of stresses are usually lower when compared to pure movements, and due to the small amount of applied force (0.5 N), the deformation effects are reduced and do not influence the accuracy of the results.

Table 1. Elastic properties of materials.

Material	Young's Modulus, E (GPa)	Poisson Ratio, ν	Refs.
Enamel	80	0.33	[7,10,11,13,24,25]
Dentin/Cementum	18.6	0.31	[7,10,11,13,24,25]
Pulp	0.0021	0.45	[7,10,11,13,24,25]
PDL	0.0667	0.49	[7,10,11,13,24,25]
Cortical bone	14.5	0.323	[7,10,11,13,24,25]
Trabecular bone	1.37	0.3	[7,10,11,13,24,25]
Bracket (stainless steel)	190	0.265	[7,10,11,13,24,25]

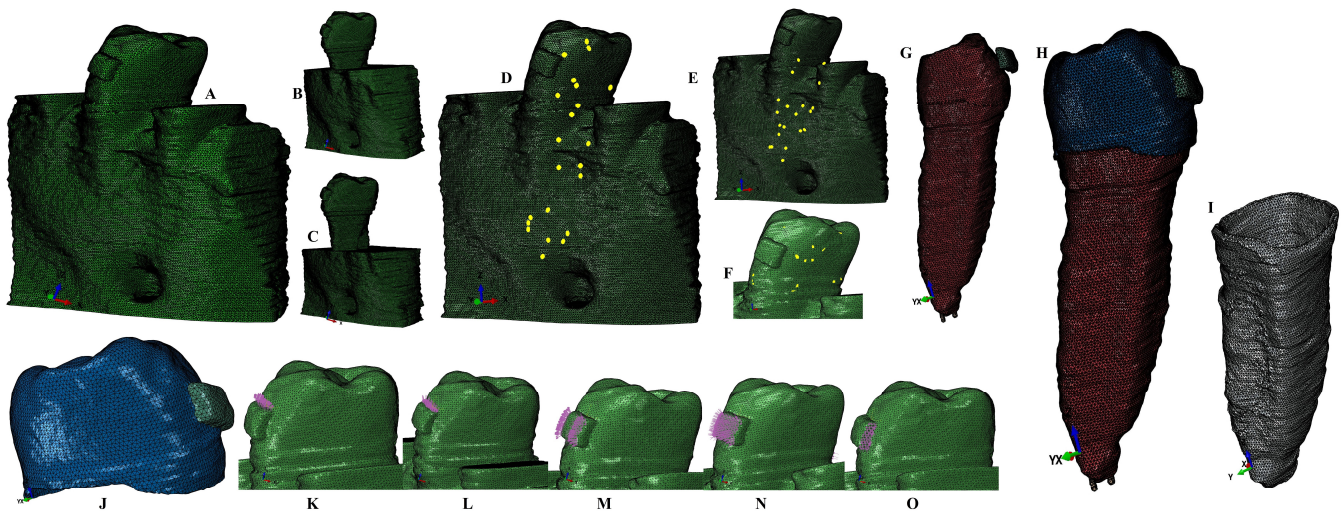


Figure 1. Mesh model: (A)—2nd lower right premolar model with intact periodontium, (B)—with 4 mm bone loss, (C)—8 mm bone loss, (D)—element warnings in dentine component, (E)—element warnings in PDL component, (F)—element warnings in bracket and enamel components, (G)—denture component (red) with dental pulp-NVB (orange) and bracket (green), (H)—tooth (enamel-blue, dentine-red) with bracket (green) and NVB (orange), (I)—PDL component (grey), (J)—enamel (blue) and bracket (green) components, (K–O) applied load vectors: (K)—extrusion, (L)—intrusion, (M)—rotation, (N)—tipping, (O)—translation.

PDL has a variable anatomical thickness of 0.15–0.225 mm and includes the neurovascular bundle of dental pulp, for each of these models [7,10,11,13,24,25], Figure 1G–I.

All the components of the tooth and surrounding support system were assembled into a 3D mesh model, keeping only the second lower premolar (other teeth being replaced by bone), with various levels of bone loss (in cervical third of PDL). Missing bone and PDL were then reconstructed, obtaining a model with intact periodontium. Thus, nine original models with intact periodontium were reconstructed following the above protocol. In each of these models, there was a simulation of a horizontal periodontal breakdown via a reduction of 1 mm of PDL and bone (from 0 to 8 mm of loss), obtaining for each of the nine intact periodontium models nine models with various levels of bone loss (totaling 81 models analyzed in the study), Figure 1A–C.

The intact periodontium models had 5.06–6.05 million C3D4 tetrahedral elements, 0.97–1.07 million nodes, and a global element size of 0.08–0.116 mm (Figure 1A). An-

other aspect that must be acknowledged (i.e., due to manual anatomical reconstruction) is the presence of a reduced number of surface anomalies/irregularities in all models (Figure 1D–F), with no error warning to be found. Thus, in Figure 1D–F, some of element warnings for one of the nine intact periodontium models were displayed: D for dentine, 22 element warnings (0.004%) from 540,969 elements; E for PDL, 20 element warnings (0.00835%) from 23,970 elements; F for enamel and bracket. 17 element warnings (0.0136%) from the 124,532 elements. Nevertheless, the quasi-continuity of the models in areas affected by stress was maintained; thus, the accuracy of the simulations was found to be high. The internal control and safety check of both software (i.e., image reconstruction and finite elements analysis) do not allow the next phase of the process to be completed if errors or too many anomalies are present, an aspect that was not seen in our study.

As in all earlier dental studies, the physical properties were linear elasticity, homogeneity, and isotropy; perfectly bonded interfaces; and model bases with zero displacements. All these properties were found acceptable because of their almost exclusive use in all earlier FEA studies and due to the fact that both applied forces (0.5 N) and displacements are extremely small [7,10,11,13,24,25].

The applied forces were of 0.5 N (approx. 50 gf) directly to the base of the bracket, simulating intrusion, extrusion, rotation, translation, and tipping (Figure 1K–O). The amount of force was selected because it is small enough to be safely applied to both intact and reduced periodontium and to produce orthodontic movements and because it allows the results obtained here to be compared with our previous FEA simulations (using the same conditions as herein) over PDL, dental pulp and NVB, and tooth [10,11,13].

The finite elements analysis totaled 405 simulations employing Abaqus 6.13–1 software (Dassault Systèmes Simulia Corp., Stationsplein 8-K, 6221 BT Maastricht, The Netherlands) and the five most used failure criteria: Von Mises (VM), Tresca (T), Maximum Principal Tensile (S1), Minimum Principal Compressive (S3), and Hydrostatic Pressure (HP).

The results were qualitatively displayed as color-coded projections of several types of stress (e.g., Figures 2–6) and quantitatively (in Table 2) as an average of stresses. These results were then correlated with previous bracket FEA studies [2–5], with those of the entire biomechanical behavior of the tooth and surrounding support tissues [10,11,13], with other tooth and PDL FEA reports [9,12,19–22,26–37]. Meanwhile, the biomechanical correctness was assessed through correlations and relationships with acknowledged clinical mechanical and materials yielding theoretical principles and properties [8,12,15,16].

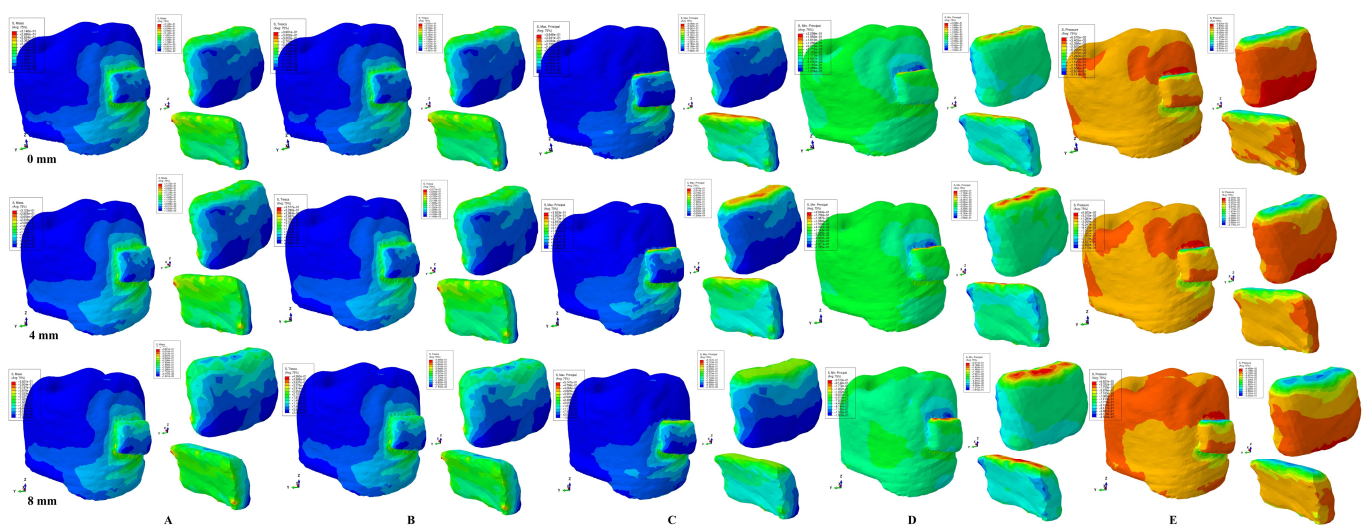


Figure 2. Comparative stress display of the five failure criteria in intact, 4 mm, and 8 mm periodontal breakdown for the extrusion movement under 0.5 N of load: (A)—Tresca, (B)—Von Mises, (C)—Max. Principal S1, (D)—Min. Principal S3, (E)—Pressure.

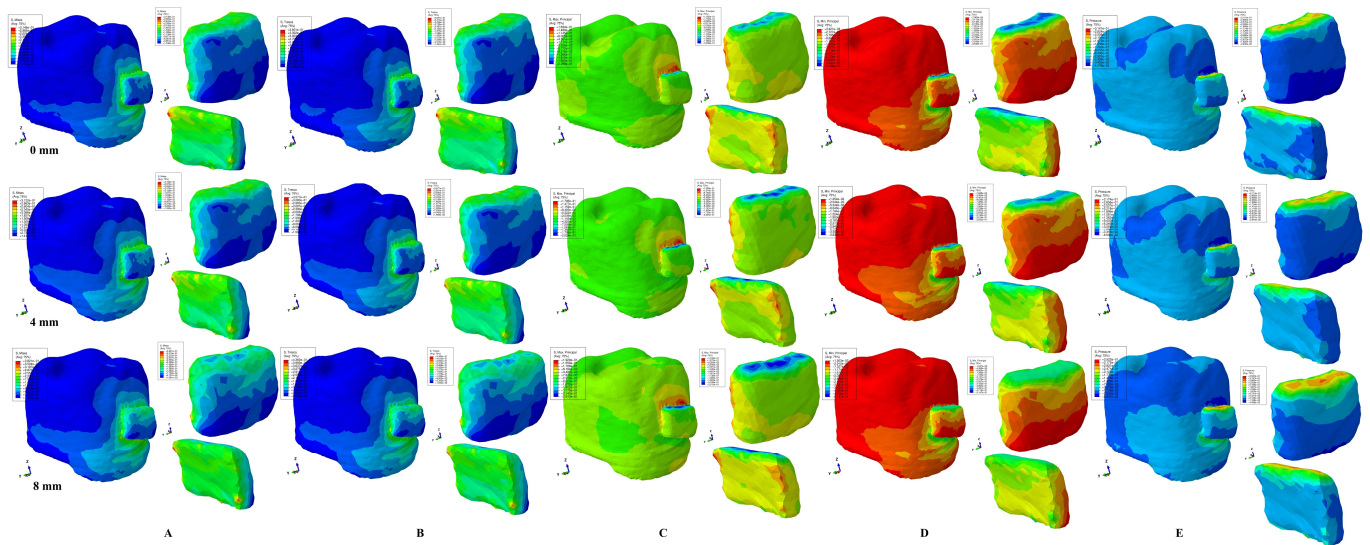


Figure 3. Comparative stress display of the five failure criteria in intact, 4 mm, and 8 mm periodontal breakdown for the intrusion movement under 0.5 N of load: (A)—Tresca, (B)—Von Mises, (C)—Max. Principal S1, (D)—Min. Principal S3, (E)—Pressure.

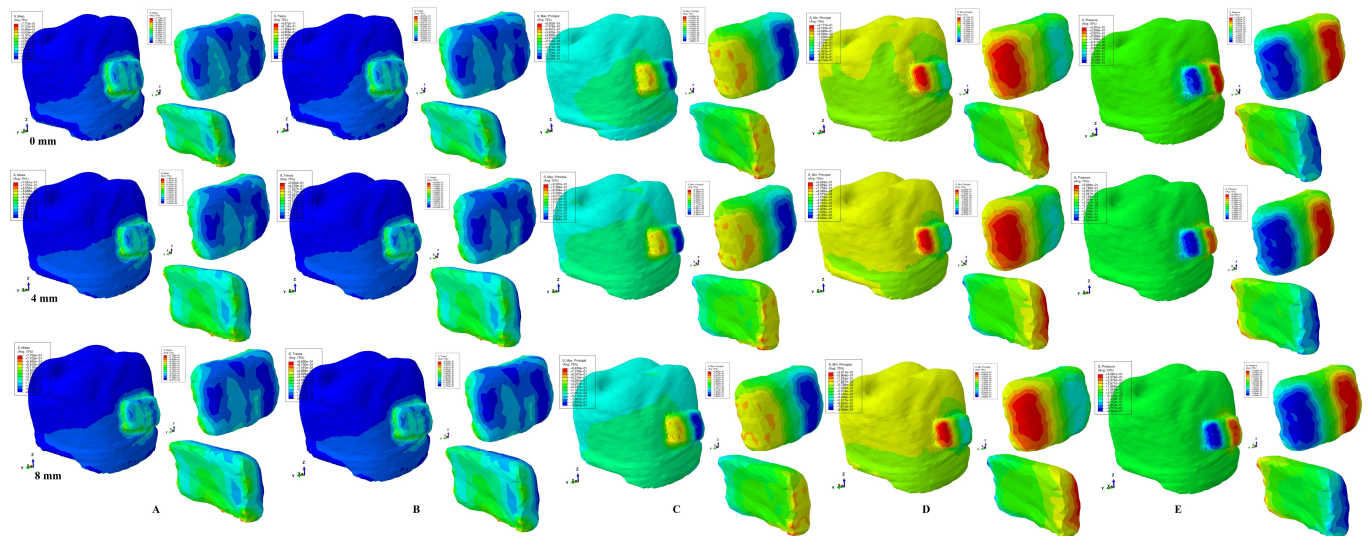


Figure 4. Comparative stress display of the five failure criteria in intact, 4 mm, and 8 mm periodontal breakdown for the rotation movement under 0.5 N of load: (A)—Tresca, (B)—Von Mises, (C)—Max. Principal S1, (D)—Min. Principal S3, (E)—Pressure.

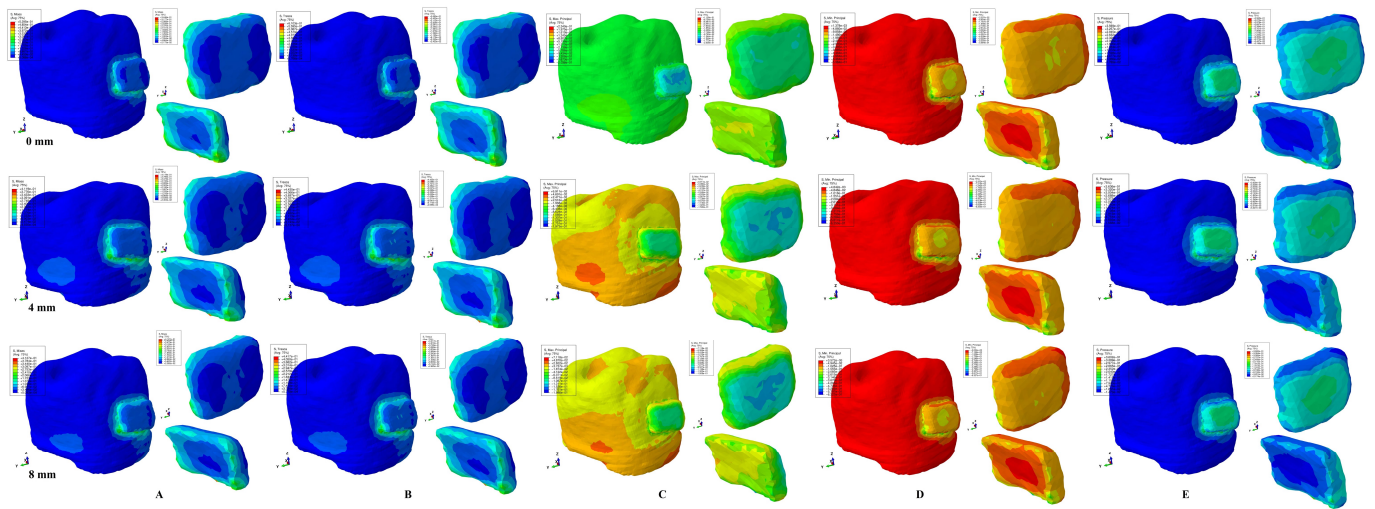


Figure 5. Comparative stress display of the five failure criteria in intact, 4 mm, and 8 mm periodontal breakdown for the tipping movement under 0.5 N of load: (A)—Tresca, (B)—Von Mises, (C)—Max. Principal S1, (D)—Min. Principal S3, (E)—Pressure.

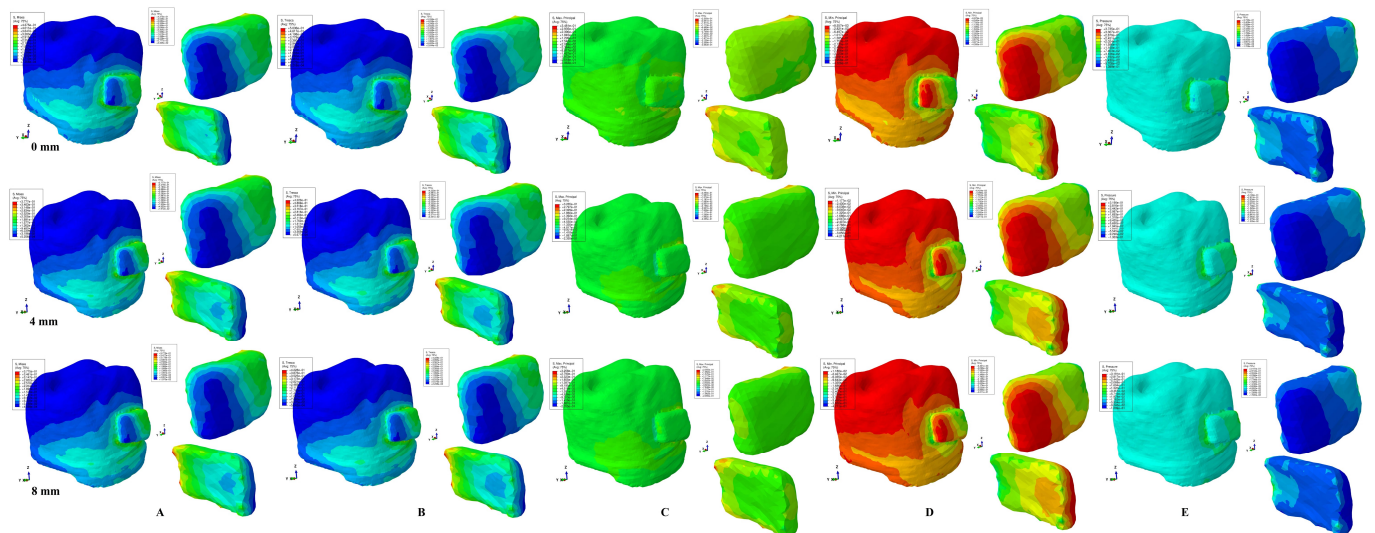


Figure 6. Comparative stress display of the five failure criteria in intact, 4 mm, and 8 mm periodontal breakdown for the translation movement under 0.5 N of load: (A)—Tresca, (B)—Von Mises, (C)—Max. Principal S1, (D)—Min. Principal S3, (E)—Pressure.

Table 2. Maximum stress average values (KPa) produced by 0.5 N of orthodontic forces.

Resorption (mm)			0	1	2	3	4	5	6	7	8
Intrusion	Tresca	E	150.94	150.94	150.94	150.94	150.03	158.45	166.60	174.70	182.93
		B	150.94	150.94	150.94	150.94	150.03	158.45	166.60	174.70	182.91
		B ext.	158.89	158.00	158.00	158.00	157.75	166.43	175.11	183.79	192.47
	VM	B int.	158.89	158.00	158.00	158.00	157.75	166.43	175.11	183.79	192.47
		E	131.92	131.92	131.92	131.92	131.95	139.06	146.17	153.28	160.39
		B	131.98	131.92	131.92	131.92	131.95	139.06	146.17	153.28	160.39
	Pressure	B ext.	138.92	138.92	138.92	138.92	138.90	146.41	153.91	161.41	168.92
		B int.	138.91	138.92	138.92	138.92	138.90	146.41	153.91	161.41	168.92
		E	92.55	100.97	109.38	117.80	126.21	130.13	134.05	137.97	141.90
		B	250.81	251.53	252.25	252.98	253.71	278.34	302.97	327.60	352.23
		B ext.	257.02	257.41	257.80	258.19	258.61	282.01	305.41	328.81	352.21
		B int.	85.80	92.25	98.70	105.15	111.63	113.86	116.09	118.32	120.56

Table 2. Cont.

Resorption (mm)		0	1	2	3	4	5	6	7	8	
S3	E	−441.82	−452.34	−462.87	−473.39	−483.92	−474.67	465.42	−456.17	−446.92	
	B	−549.31	−560.34	−571.38	−582.42	−593.45	−583.00	−572.59	−562.16	−551.74	
	B ext.	−549.31	−557.14	−564.97	−572.80	−580.63	−573.40	−566.18	−558.95	−551.74	
	B int.	−441.82	−452.34	−462.87	−473.39	−483.92	−474.67	−465.42	−456.17	−446.93	
Tipping	Tresca	E	254.60	246.45	238.30	230.15	222.01	221.81	221.61	221.41	221.21
		B	102.25	95.27	88.30	81.31	74.34	74.27	74.20	74.15	74.11
		B ext.	81.79	76.76	71.74	66.70	61.70	61.60	61.50	61.40	61.42
		B int.	225.42	219.25	213.08	206.91	200.74	200.48	200.22	199.96	199.71
	VM	E	220.92	208.73	196.55	184.37	172.19	172.19	172.19	172.19	172.31
		B	88.67	83.76	78.85	73.94	69.03	69.03	69.03	69.03	69.21
		B ext.	75.54	70.74	65.95	61.15	56.36	56.36	56.36	56.36	56.22
		B int.	210.16	195.96	181.77	167.57	153.38	153.38	153.38	153.38	153.41
	Pressure	E	138.49	138.96	139.44	139.92	140.40	140.69	140.99	141.29	141.59
		B	138.49	138.96	139.44	139.92	140.40	140.69	140.99	141.29	141.59
		B ext.	122.30	122.93	123.56	124.19	124.82	124.90	124.98	125.06	125.14
		B int.	63.75	63.43	63.12	62.81	62.50	62.24	61.99	61.73	61.48
S1	E	−130.11	−130.11	−130.11	−130.11	−130.80	−131.08	−131.08	−131.08	−131.18	
	B	−130.81	−130.11	−130.11	−130.11	−130.86	−131.08	−131.08	−131.08	−131.11	
	B ext.	−124.46	−126.44	−128.43	−130.41	−132.40	−132.40	−132.40	−132.40	−132.37	
	B int.	−71.46	−72.69	−73.93	−75.15	−76.39	−76.39	−76.39	−76.39	−76.77	
S3	E	−398.51	−403.92	−409.34	−414.75	−420.17	−420.17	−420.17	−420.17	−420.61	
	B	−148.61	−150.24	−151.87	−153.50	−155.14	−155.14	−155.14	−155.14	−155.57	
	B ext.	−164.91	−167.51	−170.11	−172.71	−175.31	−175.31	−175.31	−175.31	−175.36	
	B int.	−164.91	−167.51	−170.11	−172.71	−175.31	−175.31	−175.31	−175.31	−173.61	

E—enamel; B—bracket; B ext.—external side of bracket; B int.—internal side of bracket.

3. Results

The results of this analysis (Figures 2–6, Table 2) are based on a total of 405 FEA simulations. No differences related to gender, periodontal status, or age were seen.

From a qualitative point of view (i.e., color-coded projections), all five types of failure criteria displayed higher stress areas on and around the bracket area, Figures 2–6. The stress distribution areas remained the same (with some small particularities) independently of levels of bone loss, suggesting that periodontal breakdown does not change the stress distribution pattern from 0 to 8 mm of tissue loss. As expected, the maximum stress areas were displayed on sites/surfaces of applied force, on the internal surface of the brackets, and on the enamel around the bracket area. The Von Mises (maximum overall/equivalent stress) and Tresca (maximum shear stress) criteria displayed similar stresses and visible distribution patterns for all five movements and periodontal breakdown levels (0–8 mm), opposite to the other three failure criteria (Maximum Principal Tensile stress, Minimum Principal Compressive stress, and Hydrostatic Pressure).

From a quantitative point of view (i.e., average numerical values in KPa), all five types of failure criteria showed comparable results, Table 2. Hydrostatic pressure criteria displayed the lowest values among all five criteria. The amount of stress displayed on the bracket (internal surface and force appliance site/surface) was higher than that displayed in the enamel component. Based on the quantitative results, rotation and translation movements seem to be the most stressful among all five types. During simulated bone loss, both T and VM showed a small variation (less than 10%) in the amounts of stress: a light increase for intrusion and extrusion, a light decrease for translation and tipping, and consistent results for rotation. The light variations were also seen for the other three criteria: a general slight increase for intrusion and extrusion and a decrease for translation; for rotation, a decrease for S1 and HP and an increase for S3; and for tipping, an increase for S1 and S3 and a decrease for HP. The quantitative results (stress displayed) of the simulations for enamel (in KPa) in this study were lower than those reported for enamel (in MPa) for maximum compressive stress of 62.2 MPa (premolars and canines) [8], maximum tensile strength of 11.5–42.1 MPa (third molar) [15], and maximum shear stress of 53.9–104 MPa (third maxillary molar) [16].

This analysis aimed to assess stress distribution of the five most used orthodontic light forces in the stainless-steel bracket and enamel component of the tooth. Additionally, the biomechanical changes in the stress distribution during a gradual horizontal breakdown process from 0 to 8 mm were assessed. The present assessment was the result of an FEA employing five of the most used failure criteria, also aiming to select the most exact one in supplying trustworthy results.

It must be emphasized that all failure criteria to be employed in the FEA are designed to accurately describe the biomechanical behavior of a certain type of material (i.e., brittle, ductile, gas, or liquid). Thus, their employment without assessing the type of material and the internal micro-architecture the analyzed structure is made of could lead to incorrect results [7,10–13]. The main difference between the design of different failure criteria is related to the biomechanical behavior of the material when subjected to forces (i.e., the yielding of materials theory—the ability to absorb mechanical overload).

As is common knowledge in the engineering field of materials science, a ductile material (e.g., steel, rubber, platinum, copper) suffers from several types of elastic and/or plastic deformation (recoverable/non-recoverable) before rupture/destruction occurs when subjected to tensile and compressive stress [7,10,11,13,24,25]. The type of deformation consequences cannot be changed by simply dropping the applied force. Firstly, elastic deformation occurs, the effects of which disappear when the force is removed, and the object returns to its original shape (recoverable). Secondly, if the amount of tensile stress increases, plastic deformation occurs (i.e., in the strain hardening region closely followed by the necking region), resulting in the fracture/rupture of the material. The pre-fracture state of necking is shown by the reduction in cross-sectional area, beginning after the ultimate strength is reached, so the material can no longer withstand the maximum stress. The application of compressive stress to materials leads to their shortening, such that when the maximum compressive strength is reached, buckling (sudden change in form/shape under deformation) and then structural failure occurs. The yielding point is the limit moment of elastic behavior and the beginning of the plastic one. Below the yielding point, the material will suffer from elastic deformation (returning to original form if stress is removed), while if this yielding point is passed, the deformation will be permanent and non-reversible, ending with the fracture of material. Polymers are also considered as ductile materials suffering from plastic deformation.

Brittle materials (e.g., glass, stone, clay, concrete, cast iron) suffer from extremely small deformations (usually non-recoverable) before fracture/destruction occurs. There are also materials that have a more ductile behavior depending upon the temperature (i.e., higher or lower) called thermoplastic materials (soft and hard). Soft thermoplastic materials suffer from a wide range of plastic deformation (i.e., copper, gold, steel, rubber). Hard thermoplastics suffer a minimal plastic deformation (e.g., plastic, rubber, crystal).

For liquids/gas, pressure criteria were specially designed since there are no shear stresses in their biomechanical behavior.

The internal structure of materials (i.e., homogenous, non-homogenous) is important in accurately describing their behavior [7,10,11,13]. For ductile materials, Tresca is designed for non-homogenous materials, while Von Mises for homogenous ones [7,10,11,13]. For brittle materials, Maximum Principal Tensile S1 and Compressive S3 stresses accurately describe their behavior. For liquids and gases, pressure criteria are suitable [7,10,11,13].

In our analysis all five of the above failure criteria were assessed. The analyzed bracket was made of stainless steel and considered a ductile material. The enamel component is a brittle material due to its micro-architecture and physical properties [8,12,15,16,18]. Nevertheless, the enamel component accounts for only an extremely small percentage of the total volume of the tooth, while all other tooth components (dentine, cementum, dental pulp, and neuro-vascular bundle) are considered of ductile resemblance. Thus, from the biomechanical point of view, the tooth structure behaves as a ductile non-homogenous material with a certain brittle mode flow, being accurately described by VM and T failure criteria [8,11,13–15]. Moreover, biomechanically speaking, a small orthodontic force

of 0.5 N produces extremely small movements able to display an almost linear-elastic behavior [10,11,13,24,25]. If brittle materials or liquid/gas criteria are used in these conditions, the biomechanical description of stress distribution and dissipation might not be entirely correct [10–13,24,25].

Previous studies [10,11,13,24,25] analyzing the description of the biomechanical behavior of the tooth and surrounding periodontium under small orthodontic forces (0.5 N) during periodontal breakdown have been reported for PDL, dental pulp, NVB, and tooth structure ductile resemblance, where only T and VM criteria are suitable (with T providing the better accuracy), while S1, S3, and HP provided inaccurate results [10,11,13]. Here, the results agree with these findings, proving that Tresca and Von Mises criteria are better suited for the analysis of stainless-steel brackets and enamel. A stress increase was also reported in the apical, middle, and cervical third of the PDL, and radicular dentine correlated with the progression of periodontal breakdown, with visible increase in color-coded stress display areas and quantitative results (all lower than MHP of 16 KPa) [10,11,13]. Herein, the results reported for T and VM showed little or no change in stress display areas during periodontal breakdown (Figures 2–6 and Table 2), since the main absorption and dissipation components of the tooth and periodontium are in the dentine–cementum structure and periodontal ligament, which agrees with clinical and biomechanical knowledge. The other three analyzed criteria showed unusual stress displays, with changes in stress distribution (increase or decrease), especially in the site of force applied to the bracket, along with the progression of periodontal loss. Nevertheless, S1, S3, and HP (despite their inaccuracies) confirmed the general behavior described by T and VM.

Thus, based on this study's qualitative and quantitative results, it seems that periodontal breakdown (0–8 mm) does not influence stress distribution in either the bracket or surrounding enamel component, which is clinically important when treating patients with periodontal disease and assessing the use of various cements for cementing steel brackets. However, during the simulated bone loss, both T and VM showed a small variation (less than 10%) in the amounts of stress: a light increase for intrusion and extrusion, a light decrease for translation and tipping, and consistent stress for rotation. These light variations were also seen for the other three criteria (Table 2). These differences in biomechanical behavior are particularly related to the reduction in periodontal support and the way movements interfere with PDL and bone (i.e., a supposing increased interference in intrusion and extrusion and a decrease in tipping and translation).

By correlating the results of this study with other reports [7,10,11,13], a clearer description of the biomechanical stress distribution and absorption during the periodontal breakdown process (i.e., 0–8 mm of loss) is provided. Periodontal support loss is highly correlated with the increase in stress, especially in the periodontal ligament (most important stresses being displayed in the cervical third). Thus, 0.5 N of force was determined the highest stress during orthodontic movements in the cervical third of PDL (nevertheless, a lower than accepted MHP value was obtained), with lower amounts of stress in the apical and middle thirds of PDL, dental pulp, and radicular dentine–cement. Rotation and translation, closely followed by tipping, seem to be the most stressful movements, especially for the periodontal ligament and NVB, with potential ischemic, resorptive, and further tissue loss risks if MHP is exceeded. The tooth's ability (i.e., dentine–cement and coronal dentine components) to absorb and dissipate the stresses produced by orthodontic forces are also confirmed (approx. 86.66–97.5% of stresses before reaching PDL, 97.56–98.25% of stresses before reaching NVB, and 99.59–99.94% before reaching dental pulp [13]).

No other studies investigating the aims of this study were found; thus, the correlations with our earlier reports were the only possibility and thus necessary [10,11,13].

Few studies [1–6] about the analysis of stress distribution (shear and tensile) in bracket were found, with FEA analyses being limited to brackets. These studies concentrated on the bracket bond's shear and tensile stress strength under excessive amounts of orthodontic forces without investigating the biomechanical behavior under light forces and the influences of intact and reduced periodontium over the stresses displayed in the surrounding

tissues (e.g., the enamel component). Another aspect seen in these studies was that despite the same applied forces being used, the stress distribution in the bracket showed unexplained discrepancies.

Magesh et al. [5] (maxillary central incisor, constructed SS bracket 0.022 in. stainless-steel and titanium with 472,556 elements and 118,045 nodes) assessed the generated torque (4–28.5 N) correlated with deformations of slot walls. The quantitative wall deformations for stainless-steel were 0.3 μm top, 0.1 μm middle, and 0 μm bottom (for 4 N) and up to 44.8 μm top, 36.8 μm middle, and 9.28 μm bottom (for 28.5 N), while titanium deformed two to four times more. In both models of bracket (stainless steel and titanium), deformations were exclusively found at the slot walls, while the base of the bracket and the internal side/attachment suffered no deformation (which is biomechanically unusual, suggesting no bond failure risks and contradicting clinical-data-related knowledge). Biomechanically, the slot walls, through deformations, absorb and dissipate the applied force (e.g., an applied torque of 7.14 N generating a torque of 4 N), but there should be stress areas in the attachment side of the bracket since it transmits the movement to the tooth, while the average reported risks of bond failure are up to 28.3% [1]. Moreover, in our study, the applied force was 0.5 N (eight times lower than Magesh et al. [5]) and generated stress areas in the attachment side and entire base of the bracket, confirming stress distribution areas and risks of bond failure [1].

Elsaka et al. [3] investigated bond strength (intrusion/extrusion, translation, and tipping) of three type of brackets (stainless steel, 68,192 elements/99,487 nodes; ceramic, 73,922 elements/108,071 nodes; and titanium, 60,599 elements/80,019 nodes) on upper central incisors by qualitatively and quantitatively assessing shear stress and maximum principal stress, with (200 μm height) and without adhesive/cement. They reported that shear loading at the short side (e.g., intrusion/extrusion) of the bracket resulted in the highest bond strengths and the lowest maximum principal stress on both the cement and enamel compared with other loading modes. They also concluded that the manner of loading and choice of bracket materials influence the bond strength and stress distribution. Our results agreed with some of these reports (i.e., intrusion/extrusion movements are less harmful than rotation and translation, while the loading conditions are extremely important for stress distribution). However, their study unusually displayed stress areas located only at the edges of the bracket's internal surface, suggesting that the entire base of the bracket suffers no stress (biomechanically debatable if the yielding and failure behaviors of materials are acknowledged), which opposes our simulation results, where, with no exception, the entire surface of the bracket had various color-coded stress areas.

Algera et al. [2] (in vitro and FEA experiments) studied the shear and tensile bond strengths of metal brackets in an FEA analysis limited only to the bracket and a small enamel wall (100 N of intrusion, translation, and tipping on a stainless-steel bracket with 23,392 elements in isotropic, homogenous, and linear elasticity conditions) and reported that the stress distribution in the bracket–cement–enamel system is not homogeneous, in agreement with our results. They [2] also reported that bracket design and loading method is more important (i.e., direct correlation between loading and stress distribution) for the bond strength than the size of the bonding area, which is also in line with our research. In the color-coded stress distribution [2], the stress areas in the internal surface of bracket had various displays: For 100 N of translation, a maximum shear stress of 20.6 MPa appeared at the edge of loading side (similarly for 100 N of intrusion and 15.9 MPa), with a progressive decrease toward force-free side, which is comparable with our qualitative and quantitative results (0.384–0.5 MPa for 0.5 N of translation and 0.15 MPa for 0.5 N of intrusion). However, for 100 N tipping movement, the maximum of 25.8 MPa color-coded shear stress distribution was located only on the two short sides of the internal surface of the bracket, which opposes our simulation results, where the maximum shear stress of 0.225 MPa (for 0.5 N of force) was located in a more accurate biomechanical display around all the edges of internal surface. We assume the differences come from the loading

conditions of the investigated area (enamel wall with bracket in [2] vs. enamel crown with bracket in our simulation).

When compared (above FEA three studies), despite investigating stress distribution (shear and tensile) in the bracket bonded to a small wall of enamel, the color-coded stress distributions showed significant differences between Algera et al.'s [2] and Elsaka et al.'s [3] results (maximum stress areas in the internal surface of the bracket), as well as Magesh et al.'s [5] (maximum stress located in the slot wall). Moreover, their [2,3,5] stress distributions biomechanically showed unusual displays (i.e., concentration of the maximum stress only in a small line on the two short/long edges of the bracket, without other stress areas) when compared with a more biomechanically realistic stress display on the entire surface of the internal side in our simulations. We assume that all these differences come from the dimensions of the analyzed models (entire crown vs. a small enamel wall) that are not only more realistic simulations of clinical conditions but also takes into considerations the absorption–dissipation and stress distributions in the entire components and how these materials deform under loadings.

In Algera et al.'s [2] and Elsaka et al.'s [3] studies, loading forces were directly applied on the base of the bracket (in a similar manner as our study and with comparable results), while Magesh et al. [5] simulated the applied force directly on the bracket slot walls (with an unusual deformation limited to the slot walls). Due to difficulties in accurately reproducing clinical conditions (e.g., variability in the geometry of the slot walls, arches of various materials and geometry, cement dimensions and properties inducing a high number of variabilities and potential interferences with the accuracy of the results), the application of force directly to the base of the bracket was preferred. In our study, the construction of the bracket was performed during reconstruction of dental tissues from the CBCT images; thus, only the base of the bracket was chosen to be modeled. Both here and in earlier studies [2,3], the forces were applied in the same manner, that is, on the base of the bracket. Moreover, for a more realistic distribution of the stresses, perfectly bonded interfaces were preferred. Based on the above, we found this modeling approach acceptable, as it provided comparable results with earlier studies [2,3].

Most FEA studies assume isotropic, homogenous, and linear elasticity properties, which require certain conditions to supply correct results since biological tissues are anisotropic, non-homogeneous, and nonlinear elastic. Under low forces of up to 1 N, small displacements, and amplitude movements, all structures show linear elasticity behavior [7,10,11,13,24,25]. Nevertheless, the higher the force, the higher the displacements should be, and nonlinear elasticity would become increasingly predominant and would finally bias the FEA results. In Hemanth et al.'s [28,29] studies, the differences between linear and non-linear elastic behavior for PDL (of ductile resemblance) employing S1 and S3 brittle material failure criteria for a force up to 1 N reported that 20–50% less force was needed for non-linear vs. linear simulation. This study employed a brittle failure criteria design for describing a ductile material's biomechanical behavior, which could significantly alter the results' accuracy, since significant differences between results were reported if non-adequate failure criteria are used [10–13,24,25]. This aspect, despite not being clearly addressed in FEA studies, was visible when interpreting and correlating the results with clinical data and anatomical and physiological constants [7,10,11,13,24,25]. Thus, Field et al. [22], in an intact periodontium FEA study employing multiple failure criteria (VM, S1, S3, and HP), reported in the apical third of PDL and root multiple hydrostatic pressure stresses exceeding 16 KPa of physiological hydrostatic pressure and signaling ischemic, resorptive, and further periodontal loss risks for a tipping force of 0.35–0.5 N (which normally do not appear in clinical practice) [17]. Other FEA studies [33–37] employing hydrostatic pressure failure criteria in intact PDL reported optimal orthodontic forces of 0.28–3.31 N (but with significant differences from one study to another for the same tooth and movements, contradicting both clinical knowledge and Proffit's reports [17]), and quantitative hydrostatic pressures exceeding the physiological one by far (i.e., MPa vs. KPa). None of these studies addressed these inconsistencies that contradicted clinical knowledge,

with the only obvious explanations being non-adequate failure criteria employed, since there are reported differences for criteria analyzing the same material [12].

There are failure criteria specially designed for homogenous (Von Mises) and non-homogenous (Tresca) materials, which supply 15–30% quantitative differences when applied to the same material [7,10,11,13].

The reduced sample size of most FEA studies is another issue that must be addressed, evaluating if and how the results' accuracy is influenced. Most FEA studies (despite various failure criteria being employed) used a sample size of one (one patient, one model, few simulations) [9,12,19–23,26–37], mostly examining an idealized model of the tooth and bone. Nevertheless, we were able to draw valid conclusions from their simulations (i.e., accuracy of the results was not influenced by the reduced number of analyzed models but rather by the misuse of failure criteria, extremely high forces, or/and other boundary condition issues). FEA being based on a mathematical algorithm, the number of models is less important than the input data and boundary conditions, since the results will remain identical independently of the number of models/sample size if the information uploaded to the software suffers from bias. In our study, the sample size was nine (nine patients, eighty-one models, 405 simulations), all supplying comparable results, thus enabling us to draw valid conclusions. Moreover, the use of numerous 3D models in the FEA implies difficulties related to time consumption and computing power (the manual segmentation technique far superior in providing anatomical accuracy when compared with the automated software reconstruction method).

Far from being the most correct method in the study of tissues, FEA has numerous limitations related to the fact that it cannot accurately reproduce clinical situations (e.g., complex interactions and movements between the components of anatomical tissues, identical internal architecture of human tissues, complex associations of orthodontic movements). Additionally, more variables should be taken into careful consideration such as force levels [38] and mechanical characteristics of orthodontic wires [39]. Thus, correlating FEA results with *in vivo* and *in vitro* studies for a better image of the biomechanical behavior of tissues is of importance. Nevertheless, FEA is the only possible method that provides a detailed individualized analysis for each anatomical component of the tissues (i.e., not allowed by other methods that supply a general view).

4. Conclusions

1. The Tresca (found to be better suited) and Von Mises criteria are more correct (qualitatively) than the other three criteria in both intact and reduced periodontium in the study of stress distribution in stainless-steel brackets.
2. Qualitatively, the Tresca and Von Mises criteria simulations with 0.5 N of force and five orthodontic movements generated the maximum stress areas in the attachment side and the entire base of the bracket, confirming non-homogenous stress distribution areas and risks of bond failure.
3. Qualitatively, for all five failure criteria, maximum stress areas were displayed on the applied force site/surface, on the internal surface of the bracket, and in the enamel around bracket area in a non-homogenous manner.
4. Quantitatively, all five types of failure criteria showed comparable results, with higher amounts of stress displayed on the bracket (internal surface and force appliance site/surface) when compared with the enamel component.
5. All five failure criteria quantitatively showed rotation and translation, closely followed by tipping to be the most stressful movements.
6. In all five failure criteria's simulations rotation, translation and tipping movements showed slightly lower quantitative values for 8 mm bone loss when compared with intact periodontium, while intrusion and extrusion has shown the opposite behavior (i.e., a slight increase).
7. The periodontal breakdown has little to no influence over the stress display in the bracket and surrounding enamel area for all five orthodontic movements.

Author Contributions: Conceptualization: R.A.M.; Methodology: R.A.M.; Software: R.A.M., S.M.B. and M.D.B.; Validation: R.A.M., A.G.D., S.M.B., M.D.B. and C.D.O.; Formal analysis: R.A.M., M.D.B. and S.M.B.; Investigation: R.A.M. and S.M.B.; Resources: R.A.M.; Data Curation: R.A.M.; Writing—original draft preparation: R.A.M.; Writing—review and editing: R.A.M., A.G.D. and C.D.O.; Visualization, Supervision, and Project administration: R.A.M., A.G.D. and C.D.O.; Funding acquisition: R.A.M., A.G.D. and C.D.O. All authors have read and agreed to the published version of the manuscript.

Funding: The authors were the funders of this research project.

Institutional Review Board Statement: The research protocol has been approved by the Ethical Committee of the University of Medicine (158/2.04.2018).

Informed Consent Statement: Informed oral consent was obtained from all subjects involved in the study.

Conflicts of Interest: The authors declare that they have no conflict of interest.

References

- Eser, I.; Cicek, O.; Ozkalayci, N.; Yetmez, M.; Erenner, H. Effect of Different Types of Adhesive Agents on Orthodontic Bracket Shear Bond Strength: A Cyclic Loading Study. *Materials* **2023**, *16*, 724. [[CrossRef](#)] [[PubMed](#)]
- Algera, T.J.; Feilzer, A.J.; Prah-Andersen, B.; Kleverlaan, C.J. A comparison of finite element analysis with in vitro bond strength tests of the bracket-cement-enamel system. *Eur. J. Orthod.* **2011**, *33*, 608–612. [[CrossRef](#)] [[PubMed](#)]
- Elsaka, S.E.; Hammad, S.M.; Ibrahim, N.F. Evaluation of stresses developed in different bracket-cement-enamel systems using finite element analysis with in vitro bond strength tests. *Prog. Orthod.* **2014**, *15*, 33. [[CrossRef](#)] [[PubMed](#)]
- Kumar, A.A.; Sekar, S.; Kumar, S.S.; Divakar, G.; Vijayarangam, K.; Arulsevi, S. Computation and Collation of Torque Expression in 0.018 Inch and 0.022 Inch Preadjusted Bracket Slots on Passive Insertion of Full-Size Archwire: A Finite Element Study. *J. Pharm. Bioallied Sci.* **2022**, *14* (Suppl. S1), S143–S147. [[CrossRef](#)] [[PubMed](#)]
- Magesh, V.; Hari Krishnan, P.; Kingsly Jeba Singh, D. Finite element analysis of slot wall deformation in stainless steel and titanium orthodontic brackets during simulated palatal root torque. *Am. J. Orthod. Dentofac. Orthop. Off. Publ. Am. Assoc. Orthod. Its Const. Soc. Am. Board Orthod.* **2018**, *153*, 481–488. [[CrossRef](#)] [[PubMed](#)]
- Magesh, V.; Hari Krishnan, P.; Singh, D.K.J. Experimental evaluation of orthodontic bracket slot deformation to simulated torque. *Proc. Inst. Mech. Eng. Part H J. Eng. Med.* **2021**, *235*, 940–946. [[CrossRef](#)] [[PubMed](#)]
- Moga, R.A.; Olteanu, C.D.; Botez, M.D.; Buru, S.M. Assessment of the Orthodontic External Resorption in Periodontal Breakdown—A Finite Elements Analysis (Part I). *Healthcare* **2023**, *11*, 1447. [[CrossRef](#)] [[PubMed](#)]
- Chun, K.; Choi, H.; Lee, J. Comparison of mechanical property and role between enamel and dentin in the human teeth. *J. Dent. Biomech.* **2014**, *5*, 1758736014520809. [[CrossRef](#)]
- Maravić, T.; Comba, A.; Mazzitelli, C.; Bartoletti, L.; Balla, I.; di Pietro, E.; Josić, U.; Generali, L.; Vasiljević, D.; Blažić, L.; et al. Finite element and in vitro study on biomechanical behavior of endodontically treated premolars restored with direct or indirect composite restorations. *Sci. Rep.* **2022**, *12*, 12671. [[CrossRef](#)]
- Moga, R.A.; Buru, S.M.; Olteanu, C.D. Assessment of the Best FEA Failure Criteria (Part I): Investigation of the Biomechanical Behavior of PDL in Intact and Reduced Periodontium. *Int. J. Environ. Res. Public Health* **2022**, *19*, 12424. [[CrossRef](#)]
- Moga, R.A.; Buru, S.M.; Olteanu, C.D. Assessment of the Best FEA Failure Criteria (Part II): Investigation of the Biomechanical Behavior of Dental Pulp and Apical-Neuro-Vascular Bundle in Intact and Reduced Periodontium. *Int. J. Environ. Res. Public Health* **2022**, *19*, 15635. [[CrossRef](#)]
- Perez-Gonzalez, A.; Iserte-Vilar, J.L.; Gonzalez-Lluch, C. Interpreting finite element results for brittle materials in endodontic restorations. *Biomed. Eng. Online* **2011**, *10*, 44. [[CrossRef](#)]
- Moga, R.A.; Olteanu, C.D.; Daniel, B.M.; Buru, S.M. Finite Elements Analysis of Tooth—A Comparative Analysis of Multiple Failure Criteria. *Int. J. Environ. Res. Public Health* **2023**, *20*, 4133. [[CrossRef](#)] [[PubMed](#)]
- Jang, Y.; Hong, H.T.; Roh, B.D.; Chun, H.J. Influence of apical root resection on the biomechanical response of a single-rooted tooth: A 3-dimensional finite element analysis. *J. Endod.* **2014**, *40*, 1489–1493. [[CrossRef](#)]
- Giannini, M.; Soares, C.J.; de Carvalho, R.M. Ultimate tensile strength of tooth structures. *Dent. Mater. Off. Publ. Acad. Dent. Mater.* **2004**, *20*, 322–329. [[CrossRef](#)] [[PubMed](#)]
- Konishi, N.; Watanabe, L.G.; Hilton, J.F.; Marshall, G.W.; Marshall, S.J.; Staninec, M. Dentin shear strength: Effect of distance from the pulp. *Dent. Mater. Off. Publ. Acad. Dent. Mater.* **2002**, *18*, 516–520. [[CrossRef](#)] [[PubMed](#)]
- Proffit, W.R.; Fields, H.W.; Sarver, D.M.; Ackerman, J.L. *Contemporary Orthodontics*, 5th ed.; Elsevier: St. Louis, MO, USA, 2012.
- Kailasam, V.; Rangarajan, H.; Easwaran, H.N.; Muthu, M.S. Proximal enamel thickness of the permanent teeth: A systematic review and meta-analysis. *Am. J. Orthod. Dentofac. Orthop. Off. Publ. Am. Assoc. Orthod. Its Const. Soc. Am. Board Orthod.* **2021**, *160*, 793–804.e3. [[CrossRef](#)] [[PubMed](#)]

19. Gupta, M.; Madhok, K.; Kulshrestha, R.; Chain, S.; Kaur, H.; Yadav, A. Determination of stress distribution on periodontal ligament and alveolar bone by various tooth movements—A 3D FEM study. *J. Oral Biol. Craniofacial Res.* **2020**, *10*, 758–763. [[CrossRef](#)]
20. Shaw, A.M.; Sameshima, G.T.; Vu, H.V. Mechanical stress generated by orthodontic forces on apical root cementum: A finite element model. *Orthod. Craniofacial Res.* **2004**, *7*, 98–107. [[CrossRef](#)]
21. Merdji, A.; Mootanah, R.; Bachir Bouiadjra, B.A.; Benaissa, A.; Aminallah, L.; Ould Chikh, E.B.; Mukdadi, S. Stress analysis in single molar tooth. *Mater. Sci. Eng. C Mater. Biol. Appl.* **2013**, *33*, 691–698. [[CrossRef](#)]
22. Field, C.; Ichim, I.; Swain, M.V.; Chan, E.; Darendeliler, M.A.; Li, W.; Li, Q. Mechanical responses to orthodontic loading: A 3-dimensional finite element multi-tooth model. *Am. J. Orthod. Dentofac. Orthop. Off. Publ. Am. Assoc. Orthod. Its Const. Soc. Am. Board Orthod.* **2009**, *135*, 174–181. [[CrossRef](#)] [[PubMed](#)]
23. Huang, L.; Nemoto, R.; Okada, D.; Shin, C.; Saleh, O.; Oishi, Y.; Takita, M.; Nozaki, K.; Komada, W.; Miura, H. Investigation of stress distribution within an endodontically treated tooth restored with different restorations. *J. Dent. Sci.* **2022**, *17*, 1115–1124. [[CrossRef](#)] [[PubMed](#)]
24. Moga, R.A.; Olteanu, C.D.; Botez, M.; Buru, S.M. Assessment of the Maximum Amount of Orthodontic Force for Dental Pulp and Apical Neuro-Vascular Bundle in Intact and Reduced Periodontium on Bicuspid (Part II). *Int. J. Environ. Res. Public Health* **2023**, *20*, 1179. [[CrossRef](#)] [[PubMed](#)]
25. Moga, R.A.; Olteanu, C.D.; Botez, M.; Buru, S.M. Assessment of the Maximum Amount of Orthodontic Force for PDL in Intact and Reduced Periodontium (Part I). *Int. J. Environ. Res. Public Health* **2023**, *20*, 1889. [[CrossRef](#)]
26. Vikram, N.R.; Senthil Kumar, K.S.; Nagachandran, K.S.; Hashir, Y.M. Apical stress distribution on maxillary central incisor during various orthodontic tooth movements by varying cemental and two different periodontal ligament thicknesses: A FEM study. *Indian J. Dent. Res. Off. Publ. Indian Soc. Dent. Res.* **2012**, *23*, 213–220. [[CrossRef](#)] [[PubMed](#)]
27. McCormack, S.W.; Witzel, U.; Watson, P.J.; Fagan, M.J.; Groning, F. Inclusion of periodontal ligament fibres in mandibular finite element models leads to an increase in alveolar bone strains. *PLoS ONE* **2017**, *12*, e0188707. [[CrossRef](#)]
28. Hemanth, M.; Deoli, S.; Raghuvver, H.P.; Rani, M.S.; Hegde, C.; Vedavathi, B. Stress Induced in the Periodontal Ligament under Orthodontic Loading (Part I): A Finite Element Method Study Using Linear Analysis. *J. Int. Oral Health JIOH* **2015**, *7*, 129–133. [[PubMed](#)]
29. Hemanth, M.; Deoli, S.; Raghuvver, H.P.; Rani, M.S.; Hegde, C.; Vedavathi, B. Stress Induced in Periodontal Ligament under Orthodontic Loading (Part II): A Comparison of Linear versus Non-Linear Fem Study. *J. Int. Oral Health JIOH* **2015**, *7*, 114–118.
30. Reddy, R.T.; Vandana, K.L. Effect of hyperfunctional occlusal loads on periodontium: A three-dimensional finite element analysis. *J. Indian Soc. Periodontol.* **2018**, *22*, 395–400.
31. Jeon, P.D.; Turley, P.K.; Moon, H.B.; Ting, K. Analysis of stress in the periodontium of the maxillary first molar with a three-dimensional finite element model. *Am. J. Orthod. Dentofac. Orthop. Off. Publ. Am. Assoc. Orthod. Its Const. Soc. Am. Board Orthod.* **1999**, *115*, 267–274. [[CrossRef](#)]
32. Jeon, P.D.; Turley, P.K.; Ting, K. Three-dimensional finite element analysis of stress in the periodontal ligament of the maxillary first molar with simulated bone loss. *Am. J. Orthod. Dentofac. Orthop. Off. Publ. Am. Assoc. Orthod. Its Const. Soc. Am. Board Orthod.* **2001**, *119*, 498–504. [[CrossRef](#)] [[PubMed](#)]
33. Hohmann, A.; Wolfram, U.; Geiger, M.; Boryor, A.; Kober, C.; Sander, C.; Sander, F.G. Correspondences of hydrostatic pressure in periodontal ligament with regions of root resorption: A clinical and a finite element study of the same human teeth. *Comput. Methods Programs Biomed.* **2009**, *93*, 155–161. [[CrossRef](#)] [[PubMed](#)]
34. Hohmann, A.; Wolfram, U.; Geiger, M.; Boryor, A.; Sander, C.; Faltin, R.; Faltin, K.; Sander, F.G. Periodontal ligament hydrostatic pressure with areas of root resorption after application of a continuous torque moment. *Angle Orthod.* **2007**, *77*, 653–659. [[CrossRef](#)] [[PubMed](#)]
35. Wu, J.; Liu, Y.; Li, B.; Wang, D.; Dong, X.; Sun, Q.; Chen, G. Numerical simulation of optimal range of rotational moment for the mandibular lateral incisor, canine and first premolar based on biomechanical responses of periodontal ligaments: A case study. *Clin. Oral Investig.* **2021**, *25*, 1569–1577. [[CrossRef](#)] [[PubMed](#)]
36. Wu, J.; Liu, Y.; Wang, D.; Zhang, J.; Dong, X.; Jiang, X.; Xu, X. Investigation of effective intrusion and extrusion force for maxillary canine using finite element analysis. *Comput. Methods Biomech. Biomed. Eng.* **2019**, *22*, 1294–1302. [[CrossRef](#)] [[PubMed](#)]
37. Wu, J.L.; Liu, Y.; Peng, W.; Dong, H.Y.; Zhang, J.X. A biomechanical case study on the optimal orthodontic force on the maxillary canine tooth based on finite element analysis. *J. Zhejiang Univ. Sci. B* **2018**, *7*, 535–546. [[CrossRef](#)] [[PubMed](#)]
38. Cacciafesta, V.; Sfondrini, M.F.; Lena, A.; Scribante, A.; Vallittu, P.K.; Lassila, L.V. Force levels of fiber-reinforced composites and orthodontic stainless steel wires: A 3-point bending test. *Am. J. Orthod. Dentofac. Orthop. Off. Publ. Am. Assoc. Orthod. Its Const. Soc. Am. Board Orthod.* **2008**, *133*, 410–413. [[CrossRef](#)] [[PubMed](#)]
39. Maekawa, M.; Kanno, Z.; Wada, T.; Hongo, T.; Doi, H.; Hanawa, T.; Ono, T.; Uo, M. Mechanical properties of orthodontic wires made of super engineering plastic. *Dent. Mater. J.* **2015**, *34*, 114–119. [[CrossRef](#)]

Disclaimer/Publisher’s Note: The statements, opinions and data contained in all publications are solely those of the individual author(s) and contributor(s) and not of MDPI and/or the editor(s). MDPI and/or the editor(s) disclaim responsibility for any injury to people or property resulting from any ideas, methods, instructions or products referred to in the content.